

## **MATERIAL BED COMPRESSION EXPERIMENTS AND THE EXAMINATION OF THE BULK DENSITY OF THE PRODUCT**

LÁSZLÓ TAMÁS<sup>1</sup>, ÁDÁM RÁCZ<sup>2</sup>

<sup>1</sup>*Institute of Raw Material Preparation and Environmental Processing,  
University of Miskolc  
Refra-System Ltd, Újronafő, Császárret major 10.  
laszlo.tamas@refra-system.hu*

<sup>2</sup>*Institute of Raw Material Preparation and Environmental Processing,  
University of Miskolc, ejtracz@uni-miskolc.hu*

**Abstract:** Comminution of white fused alumina (WFA) and white fused mullite (WFM) is a challenging task, as these materials have very high hardness and compression strength and are also very abrasive. Selection of the best comminution process for each particle size range thus has great importance. For this, first we must understand the effects of different types of stresses and comminution methods used for the comminution of WFA and WFM. In this article a comparison of particle size distribution and bulk density of different fractions and the influence of the applied pressure is carried out on the product of material bed compression and traditional single particle compression by roller crusher. Comminution experiments were carried out in a laboratory scale piston press to achieve material bed compression like in HPGR technology, and in an industrial scale roller crusher. The results showed that the products of the two comminution methods have a significant difference on particle size distribution and the fraction's bulk density on both materials. The effective amount (<1 mm) of the fractured particles for WFA was 72% and 74% for WFM with material bed compression comminution and with single particle compression 30% for WFA and 28% for WFM. The highest growth in the bulk density compared to the roller crusher product was achieved by material bed compression by the piston press, with 12.3% on the 0.15–0.3 mm WFA fraction.

**Keywords:** *Comminution, WFA, WFM, Material bed compression, Piston press, Roller crusher*

### **1. INTRODUCTION**

Due to the extraordinarily energy intensive processes of the raw material preparation industry, the conventional comminution and classification processes have been studied during the last few decades with the aim of decreasing the energy requirements, reducing the environmental impact, and saving money. To meet this request from the side of the manufacturing, the High-Pressure Grinding Roll technology has been studied and developed during the last 35 years [1]. The dry comminution process by HPGR first emerged in the 1980s in Germany and the basis of the technology was nearly defined by this time [2]. The main phenomenon of the HPGR comminution is

the breakage induced by particle-particle interaction. The particles of the disperse system are fed to the active comminution zone of the HPGR, where the material bed is stressed by two rotating rollers moving in opposite directions. The main difference from the conventional roller crusher is the horizontally applied high pressure, which causes highly energy efficient comminution, and the high yield of finer particles. In terms of energy utilization, the most efficient type of comminution is single particle breakage by compression loading, the second is loading the bed of particles by stress, followed by unconfined particle-bed comminution [3]. Single particle breakage can hardly be carried out continuously in operation process. Loading stress on a bed of particles can be achieved by HPGRs and unconfined particle-bed comminution by ball mills. The energetical approach of particle bed comminution was studied by German scientists. Several microprocesses take place in the particle bed during the whole comminution process, from the moment of compaction to the moments of new fragments, and their rearrangement in a new spatial distribution. Each of these processes has specific but not well-known and studied energy requirements (also with material dependence), such as energy loss due to the friction between the particles and their confinements, breakage energy, plastic deformation work, flow losses, energy loss caused by the wear of the confinements of the particle bed and energy loss due to thermoplastic effects, sound wave propagation and oscillation of elastically deformed fragments [4]. The effect of compressive stress velocity in confined particle bed comminution was studied on middle-hard limestone and hard quartz, showing that better comminution is available with the same energy absorption for the middle hard limestone. The increasing stress velocity resulted in higher energy absorption on the particle bed, but lower compression and comminution, also lower energy efficiency [5]. In another study, one of the microprocesses of comminution by stressed particle bed was examined, and that showed the flow losses of energy are only 0.1% of the total energy input in particle bed compression [6].

In an industrial environment, HPGRs were used primarily in the cement industry for the preparation of related raw materials and the dry comminution of the product, as the energy saving was a critical part of the production cost and the higher degree of energy utilization was an advantage for the low- and medium-added-value cement products [7]. Due to its successful application in the cement industry, the technology came to the attention of the mining industry and mineral raw material processing, such as diamond, copper, gold, and iron ore comminution [9–12]. Nonetheless for the HPGR applications, for ore comminution there was a difficult problem that had to be solved before these machines could be used widely: the common and severe wear on the rollers mantle by the abrasive ores. To avoid the negative consequences from comminution of more abrasive ores, the rollers mantle design was studied, and the mainly widespread and conventionally applied stud system was considered as an optimal option to reduce wear [13]. The active comminution zone of the rollers can be increased by the smaller studs, while the stress forces can be also increased, which can cause a finer product and a higher comminution ratio [13], but the higher friction due to the higher acting forces has remarkable wear too. Improved materials and casting

technology and the optimal stud system on the roller surface made it possible to build up a fine material bed, which led to lower wear due to the autogenous comminution on the rollers. In a comparison with ball mills, the major benefits of HPGRs are – for various types of minerals – better energy utilization, less selective crushing of coarse particles, and improved mineral liberation from the ores [14–15].

Generally, it can be stated that the most widespread technology is hybrid comminution, to achieve the best energy utilization and particle size reduction ratio, because the HPGRs are more efficient at lower energy inputs, and the ball mill is more efficient at higher energy inputs. Systematic experiments were carried out to examine the energy efficiency of the comminution in a HPGR-Ball Mill system and the results showed a reduction ratio of 30, costing only 70% of the energy input compared to using only a single ball mill [8].

In this article, the particle size distribution and the bulk density of WFA and WFM materials are investigated for material bed compression induced comminution by piston press, and particle breakage by two rotating surfaces in the roller crusher. The effect of the pressure applied during material bed compression is also studied and discussed in this paper.

## 2. MATERIALS AND METHODS

White fused alumina (WFA) is an excellent high-tech advanced abrasive material with a high additional value for miscellaneous applications in industrial fields such as medical and dental technology, space and aerospace industry, optical industry, and laminate industry. White fused mullite (WFM) is also a very abrasive advanced material, with a lower  $\text{Al}_2\text{O}_3$  content, which causes a lower value of mechanical strength. It has a brilliant white color, and the high purity makes it the perfect raw material for high-end ceramics and investment casting shell building.

After the melting of metallurgically pure alumina (chemical composition and properties are described in *Tables 1* and *2*) in an electric arc furnace at 2040 °C with a specific smelting work of 1.35 MWh/t, the melted WFA is casted into a mold and after solidification is over by the loss of heat, it is crushed by a jaw crusher to 0–100 mm fraction, then the roller crusher comminution results in a 0–3 mm fraction that is classified by sieves to the requested fraction. For the experiments, the pre-crushed 0–3 mm fraction was classified to 1–3 mm fraction with the particle size distribution defined in *Figure 1*; the fraction has a bulk density of 1.84 g/cm<sup>3</sup>. Sample materials are from Refra-System Ltd.

**Table 1**  
*Typical chemical composition of metallurgical grade alumina by Alumina d.o.o. Zvornik [16]*

Chemical comp.	Typical content [%]	Guaranteed limits [%]
$\text{Al}_2\text{O}_3$	98.8–99	min 98.7
$\text{SiO}_2$	0.005–0.010	max 0.015
$\text{Fe}_2\text{O}_3$	0.008–0.012	max 0.018

Chemical comp.	Typical content [%]	Guaranteed limits [%]
Na <sub>2</sub> O <sub>total</sub>	0.3–0.35	max 0.42
CaO	0.018–0.025	max 0.03
P <sub>2</sub> O <sub>5</sub>	0.0002–0.0005	max 0.0009
TiO <sub>2</sub>	0.002–0.0027	max 0.003
ZnO	0.017–0.02	max 0.022

**Table 2**

*Specification of the metallurgical grade alumina by Alumina d.o.o. Zvornik [16]*

	Typical range	Guaranteed limits
Specific Surface Area BET	75–90 [m <sup>2</sup> /g]	min 70 [m <sup>2</sup> /g]
Bulk Density	1000–1050 [kg/m <sup>3</sup> ]	max 1070 [kg/m <sup>3</sup> ]
Loss of ignition (300 °C-1000 °C)	0.6–0.9 [%]	max 1 [%]
Angle of repose	32–34 [°]	max 35 [°]
+45 microns (wet sieve)	88–95 [%]	min 85 [%]
-20 microns (wet sieve)	1–2 [%]	max 2.5 [%]

The melting process of WFM also starts with the metallurgical grade alumina powder in an electrical arc furnace with 1.2 MWh/t specific smelting work at a temperature of 1850 °C. The chemical composition can be seen in *Table 3*.

**Table 3**

*Typical chemical composition of WFM by Refra-System Ltd.*

Chemical compound	Typical content [%]
Al <sub>2</sub> O <sub>3</sub>	76.00
SiO <sub>2</sub>	23.50
Fe <sub>2</sub> O <sub>3</sub>	0.06
Na <sub>2</sub> O <sub>total</sub>	0.06
CaO	0.02
TiO <sub>2</sub>	0.02

The production of the WFM and the mechanical preparation of the fused raw material is to the same process as for the WFA. The prepared 1–3 mm fraction for the tests has a bulk density of 1.35 g/cm<sup>3</sup> and the particle size distribution shown in *Figure 1*.

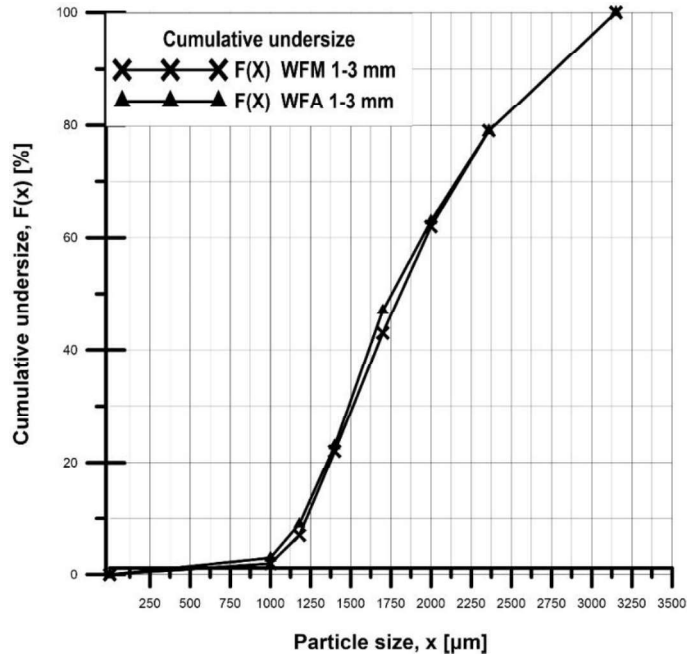


**Figure 1**

*Particle size distribution functions of 1–3 mm WFA and WFM*

The industrial scale roller crusher is a double-driven crusher by both cylinder shafts at the Refra-System Ltd. The two shafts are driven by different electrical. *Table 4* shows the geometrical and operating parameters of the roller crusher.

**Table 4**  
*Geometrical and operating parameters of the industrial scale roller crusher*

Length of the cylinders	500 mm
Diameter of the cylinders	600 mm
Material of the cylinders	Unalloyed steel
Theoretical gap size	0.5 mm
Power of the motors	11 kW; 17 kW
Feed rate	2000 kg/h

The feed material fraction was 1–3 mm WFA and WFM defined with a particle size distribution of *Figure 1*. The product of the equipment was 0–3 mm, classified into different fractions to evaluate systematically, and the roller crusher and piston press

products were compared to each other for the effectiveness of crushing and particle size reduction ratio and for the bulk densities of the different size fractions.

The laboratory hydraulic piston press was built by the Institute of Raw Material Preparation and Environmental Processing, University of Miskolc for briquetting. Two pistons are situated in the equipment, one for the pressing force transmission and one for the sample discharge. The hydraulic pressure can be adjusted to 2750 bar by the oil pressure of the piston as a maximum value. The pressing velocity can be also adjusted up to 34.5 mm/s. *Table 5* shows the technical data of the machine parameters during the measurements.

**Table 5**

*Geometrical and operating parameters of the laboratory scale piston press*

Diameter of the piston	25 mm
Piston velocity	34.5 mm/s
Pressure at Ø25 mm piston	2500–1250 bar
Material bed height	20 mm

The feed materials and their particle size distribution function were the same as specified in Figure 1, and the products were classified and measured with the same process to obtain comparable data from the two different type of comminution processes. In this measurement stage the effect of the pressure was examined with the values of 2500, 2250, 1750 and 1250 bars to the different fractions.

A TAP sieve shaker AS 200 model was used to separate the products into the required fractions developed by RETSCH. The analytical test sieve shaker is used in research and development for separation, fractioning and determination of the particle size distribution. The movement of the sieve in the equipment is a horizontal circular motion with taps. The rotational speed of the sieves was 280 min<sup>-1</sup> while the number of taps was 150 min<sup>-1</sup> during the measurements. The applied feed mass was 100 g in each case.

The bulk density of the product fractions was measured according to the MSZ 6506-84 patent standard.

### 3. RESULTS

In this section the particle size distribution of the WFA and WFM products from the feed fractions and the comparison of the bulk density of the classified fractions are presented. Also, the evaluated data from material bed comminution with different pressure levels are presented in this chapter.

Four particle size distributions can be seen in *Figure 2*, where the curves of the coarse feed are shown on the right, and on the left side the 0–3 mm product curves. Both test materials have sharply classified 1–3 mm feed fractions, with 3% and 2% of under particles for WFA and WFM.

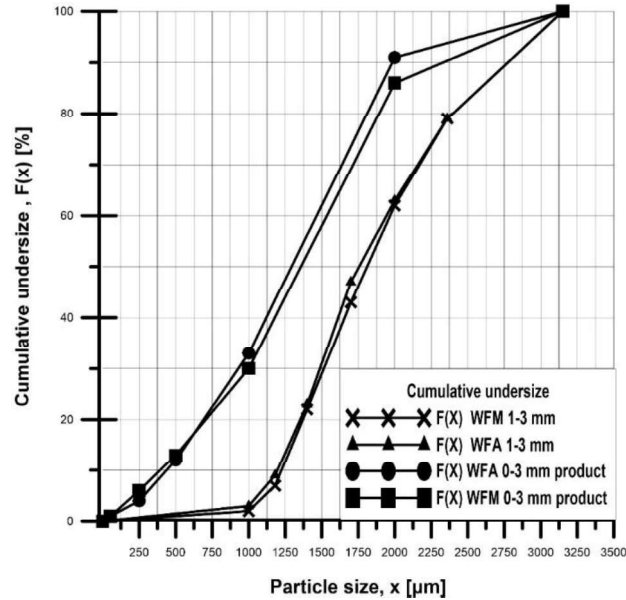


**Figure 2**

*Cumulative undersize of 1–3 mm feed and the 0–3 mm products after roller crusher*

After comminution in roller crusher, the mass ratios of the <1 mm particles were increased to 33% and 30%, respectively. This means that the effective mass of the ground particles <1 mm was 30% for WFA and 28% for WFM. Also, the size reduction can be seen at the fraction of >1 mm particles for both materials because of the horizontal shift of the cumulative undersize curves. The characteristics of the products are similar due to the similar feed fractions and stress conditions during the comminution process. The WFA product has  $x_{50} = 1.29$  mm and  $x_{80} = 1.81$  mm. The WFM product has  $x_{50} = 1.35$  mm and  $x_{80} = 1.9$  mm.

The characteristics of the piston press product were different from those of the roller crusher in for both materials. Also, it can be stated that the material bed compression produced a finer product than the roller crusher. Heineckel et al. [1] stated that the particle size distribution (PSD) of HPGR products varies from a ball mill ground product. The PSD is not only shifted along the horizontal axis of the size distribution diagram but also twist towards more fines. Tavares [17] stated that high interparticle stresses result in a much greater proportion of fine particles in comparison to conventional crushing. The mass ratio of particles <1 mm was 72% and 74% in the product. The effectively generated 0–1 mm fraction of WFA is 69% and 72% in the WFM product. The WFA product has  $x_{50} = 0.5$  mm and  $x_{80} = 1.35$  mm. The WFM product has  $x_{50} = 0.47$  mm and  $x_{80} = 1.28$  mm.

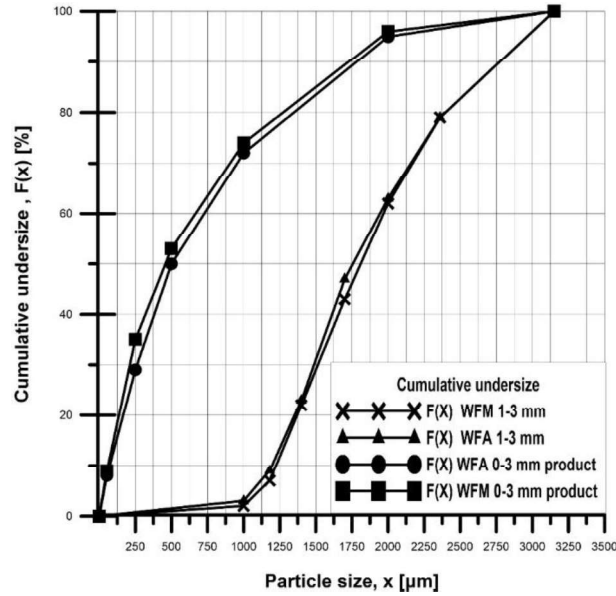


**Figure 3**

*Cumulative undersize of 1–3 mm feed and the 0–3 mm products after material bed compression*

The ratio of overground particles ( $<53 \mu\text{m}$ ) produced by the piston press is higher by 7% for WFA and 8% for WFM than the ratio produced by roller crusher, as displayed in Table 6. The horizontal shift to the finer particle size ranges from the feed particle size distribution to the product distribution can be also seen in Figure 3.

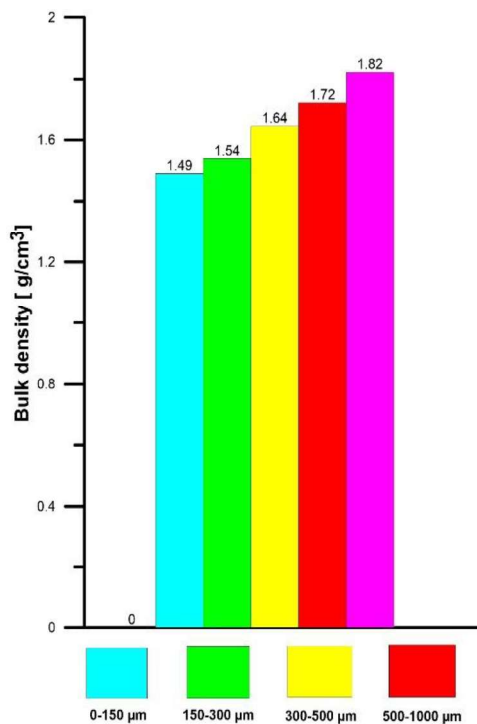
**Table 6**  
*Amount of the produced overground particles by roller crusher and piston press*

	$<53 \mu\text{m}$ [%]
WFA Roller crusher	1
WFM Roller crusher	1
WFA Piston press	8
WFM Piston press	9

The bulk density of WFA fractions produced by roller crusher can be seen in Figure 4. The product of material bed compression and roller crushing was sieved to 0–150; 150–300; 300–500; 500–1000 and 1000–2000  $\mu\text{m}$  fractions, and then the bulk density of each fraction was measured. The bulk density of the size fractions is an important parameter for the later application of the WFA and WFM products, so the comminution process should be selected according to this condition as well.

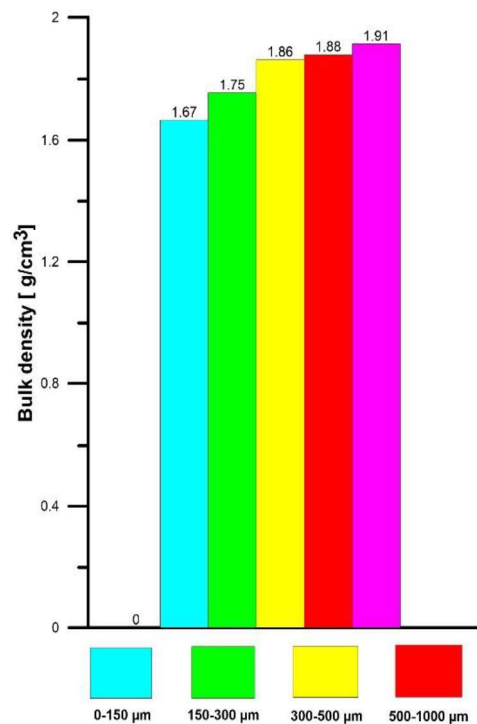


The bulk density values of the fractions of WFA roller crusher products increase with the increasing particle sizes. The minimal value of the bulk density ( $1.49 \text{ g/cm}^3$ ) can be seen in *Figure 4*, which occurred for the finest particle fraction 0–0.15 mm, and the highest bulk density ( $1.82 \text{ g/cm}^3$ ) was measured for the 1–2 mm fraction.



**Figure 4**

*Bulk density of WFA fractions produced by roller crusher*

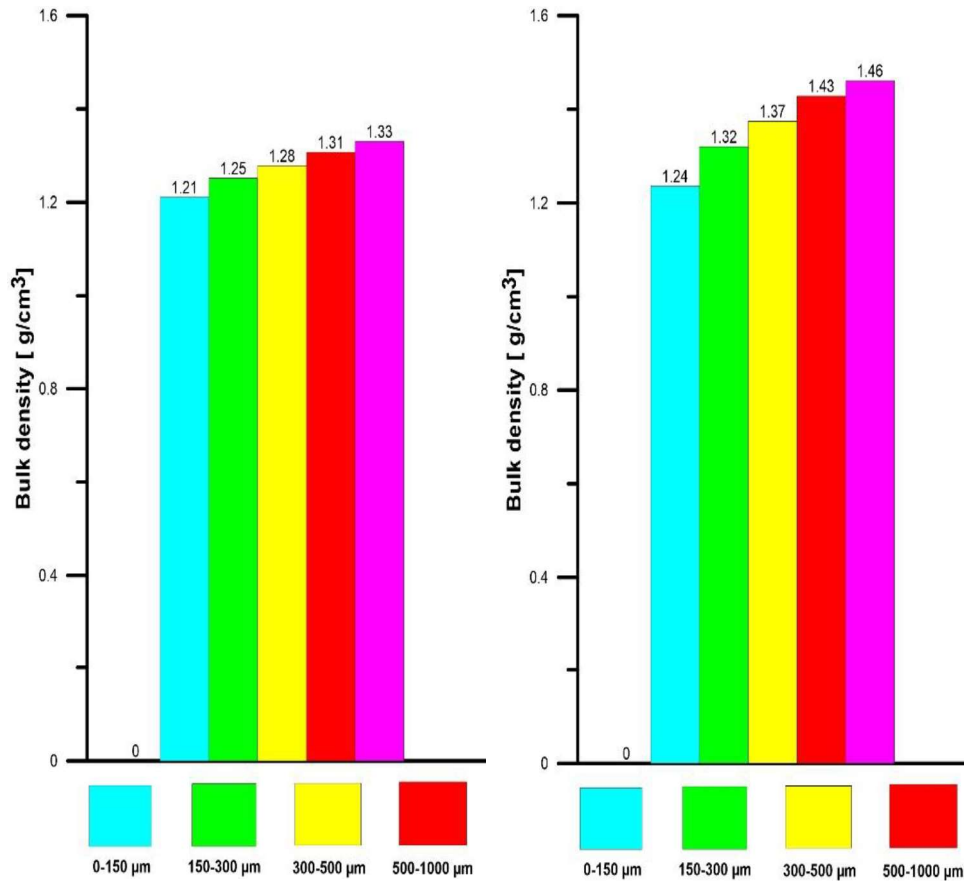


**Figure 5**

*Bulk density of WFA fractions produced by material bed compression*

An increasing tendency is also visible in the bulk density for the fractions of piston press product, with the increasing particle sizes, (*Figure 5*). Also, the finest particle size class, the 0–0.15 mm fraction, has the lowest bulk density at  $1.67 \text{ g/cm}^3$ , and the 1–2 mm fraction has the highest value at  $1.91 \text{ g/cm}^3$ . At each particle fraction the material bed compression resulted in a higher bulk density.

It can be seen in *Figure 6*, that the tendency towards higher bulk density with a coarser particle size fraction is again detectable with WFM comminution by a roller crusher, where the minimum value is  $1.21 \text{ g/cm}^3$ , and the maximum is  $1.33 \text{ g/cm}^3$ . There is less increase in the bulk density for the coarser fraction in the case of WFM due to the lower particle density of WFM ( $3.15 \text{ g/cm}^3$ ).

**Figure 6**

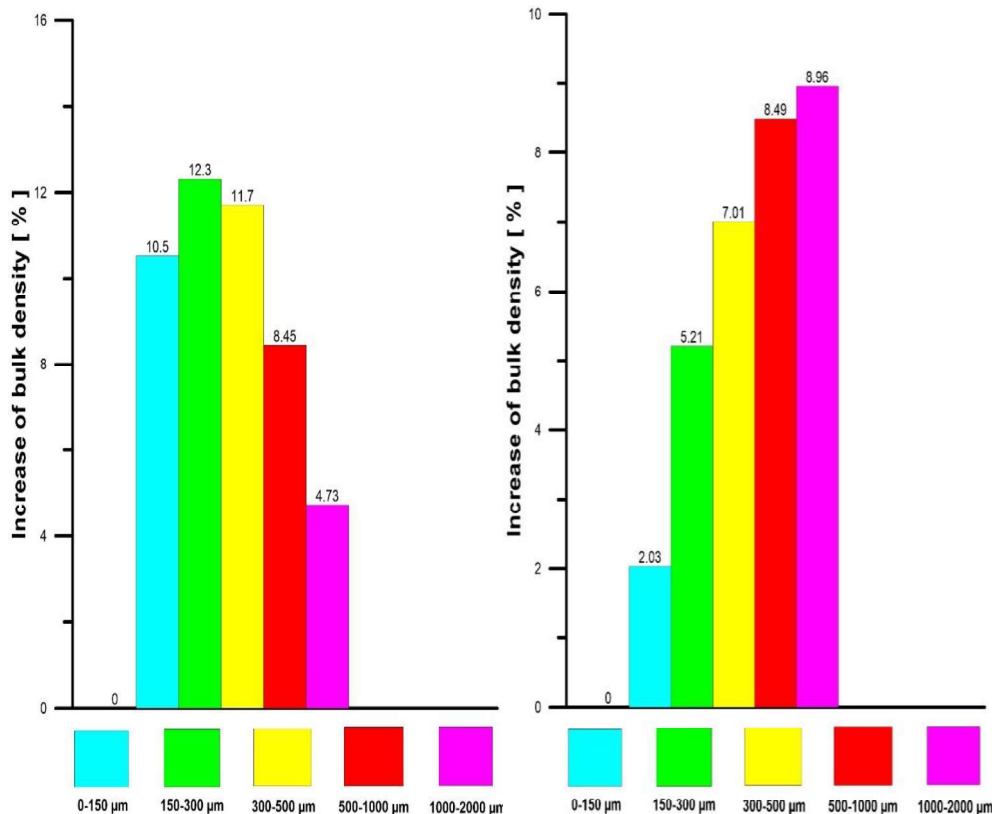
*Bulk density of WFM fractions produced by roller crusher*

**Figure 7**

*Bulk density of WFM fractions produced by piston press*

The bulk density was higher at each particle fraction, and the tendency was also increasing with the coarser particle fraction in case of the material bed compression. In *Figure 7* it can be seen that the highest bulk density of WFM was achieved by the material bed compression of the 1–2 mm fraction, with 1.46 g/cm<sup>3</sup> value, and the lowest value was 1.24 g/cm<sup>3</sup> in case of the 0–0.15 mm WFM fraction.

The increase in the bulk density of the separated WFA fractions are displayed as a percentage from the roller crusher products in *Figure 8*. The bulk density of 0.15–0.3 mm fraction has the highest increase (12.3%) in the case of the piston press product compared to application of the roller crusher.

**Figure 8**

*Bulk density of WFA fractions  
produced by piston press  
(Basic value; Roller crusher)*

**Figure 9**

*Bulk density of WFM fractions  
produced by piston press  
(Basic value; Roller crusher)*

The peak value is for the 0.15–0.3 mm fraction, then the increase in the bulk density becomes less prominent with the coarser fractions. The maximum growth (12.3%) was achieved with WFA according to the higher maximal specific gravity (4.1 g/cm<sup>3</sup>).

The increased bulk density values for the material bed compression at the piston press are represented with the same methodology as for WFM. *Figure 9* shows that with a coarser fraction, the growth in the bulk density becomes higher, and the maximum value is 8.96% on the 1–2 mm fraction, while the lowest growth is 2.03% on the 0–0.15 mm fraction.

*Figure 10* shows the effect of the reduced pressures on the material bed of WFA, i.e., how the fines of the products changes. The overground particles <53 µm, from 8% with the applied pressure of 2500 bar started to decrease with the lower applied pressure. With half of the pressure the overground particles fraction reached only

3.9%, while the reduction ratio is still good because the 0–1 mm fraction in the product is 63%. That also means with the reduced applied pressure from 2500 to 1250 bar, produced 51% less overgrounded particles, but at the same time the 0–1 mm fraction in the product from the feed 1–3 mm is still decreased by only 12.5%.

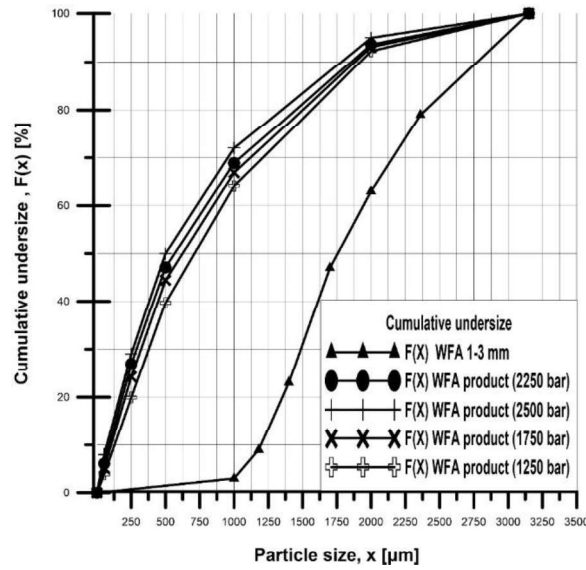


Figure 10

Effect of pressure on the material bed compression for WFA

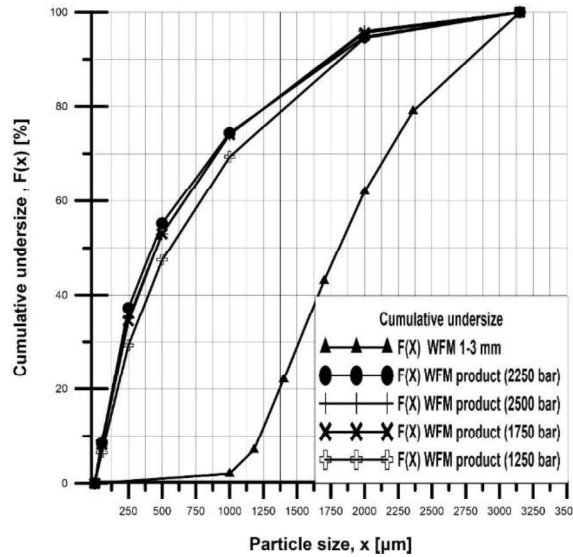


Figure 11

Effect of pressure on the material bed compression for WFM

The particle size distribution of the feed material and the products is shown in *Figure 11*. It can be seen that the amount of the overground particles decreased from 9% to 6.5% with half of the applied pressure of 2500 bar. The 0–1 mm fraction in the products changes from 72% to 69% with 2500 and 1250 bar pressure. This means only a 5% decrease in the 0–1 mm fraction production while the amount of the overground particles is less by 28%.

#### 4. CONCLUSIONS

In the present study, the comminution of WFA and WFM by compression in roller crusher and material bed compression using a piston press was investigated. The particle size distribution and bulk density of the products were determined and compared. The effectiveness of comminution by material bed compression has already been proven by several authors [7, 9–12] and is also supported by the present measurement results. Comminution with the piston press by material bed compression produced 72% (WFA) and 74% (WFM) 0–1 mm fraction from the 1–3 mm feed fraction, while that produced by the roller crusher contained only 30% (WFA) and 28% (WFM). That means 2.4 times more desired product particles in WFA and 2.6 times more in WFM product compared to material bed compression. The overground <53  $\mu\text{m}$  particles were 8% in WFA and 9% in WFM products with material bed compression in the piston press with the applied pressure of 2500 bar. The roller crusher product contained only 1% <53  $\mu\text{m}$  particle.

The coarser product fractions had higher bulk density values using the piston press and roller crusher for both materials. The results showed that each fraction of WFA and WFM produced by material bed compression had a higher bulk density. The stress environment in the material bed showed that the rigid WFA and WFM particles effectively transmit the energy. Applied pressure as an optional way to reduce the amount of overground <53  $\mu\text{m}$  particles showed good results. Using 1250 bar instead of 2500 bar by the piston press resulted in 51% less overground particles for WFA, while the yield of the 0–1 mm fraction decreased only by 12.5%. WFM showed similar results for the analogical tests, with the amount of particles <53  $\mu\text{m}$  was reduced by 28%, and only a 5% mass decrease of the 0–1 mm fraction recorded.

The measurement results proved that material bed compression is more effective than simple particle compression as a comminution method for 1–3 mm WFA and WFM products in order to create high density product fractions.

#### REFERENCES

- [1] Heinicke, F., Günter, H., Lieberwirth, H. (2016). *Modelling of HPGR Edge recycling with progressive grinding data*. [https://www.koepfern-international.com/fileadmin/user\\_upload/downloads/Comminution/Paper\\_HPGR\\_edge\\_recycling\\_02-2016.pdf](https://www.koepfern-international.com/fileadmin/user_upload/downloads/Comminution/Paper_HPGR_edge_recycling_02-2016.pdf).

- 
- [2] Schönert, K. (1966). *Einzelkorn-Druckzerkleinerung und Zerkleinerungskinetik. Untersuchungen an Kalkstein-, Quarz-, und Zementklinkerkörnern des Größenbereiches 0,1–0,3mm*. Dissertation. TH Karlsruhe, 1966
- [3] Schönert, K. (1979). Energetische Aspekte des Zerkleinerns spröder Stoffe. *Zement-Kalk-Gips*. Int. 32, 1–9.
- [4] Schubert, H. (1967). Zu einigen Fragen der Kollektivzerkleinerung. *Chem. Technol.*, 19, pp. 595–598.
- [5] Mütze, T., Husemann, K. (2008). Compressive stress: Effect of stress velocity on confined particle bed comminution. *Chem. Eng. Res. Des.*, 86, pp. 379–383, <https://doi.org/10.1016/j.cherd.2007.11.007>.
- [6] Mütze, T. (2015). Energy dissipation in particle bed comminution. *International Journal of Mineral Processing*, 136 pp. 15–19. <http://dx.doi.org/10.1016/j.minpro.2014.10.004>
- [7] Camalan, M., Önal, M. A. R. (2016). Influence of high-pressure grinding rolls on physical properties and impact breakage behavior of coarsely sized cement clinker. *Part. Sci. Technol.*, 34, pp. 278–288. <https://doi.org/10.1080/02726351.2015.1075636>
- [8] Fuerstenau, D. W., Kapur, P. C., Schönert, K., Marktscheffel, M. (1990). Comparison of Energy Consumption in the Breakage of Single Particles in a Rigidly Mounted Roll Mill with Ball Mill Grinding. *Int. J. Miner. Process.*, 28, pp. 109–125, [https://doi.org/10.1016/0301-7516\(90\)90030-3](https://doi.org/10.1016/0301-7516(90)90030-3).
- [9] Abazarpoor, A., Halali, M., Hejazi, R., Saghaeian, M. (2018). HPGR effect on the particle size and shape of iron ore pellet feed using response surface methodology. *Miner. Process. Extr. Metall. Trans. Inst. Min. Metall.*, 127, pp. 40–48, <https://doi.org/10.1080/03719553.2017.1284414>.
- [10] Anticoi, H., Guasch, E., Hamid, S., Oliva, J., Alfonso, P., Garcia-Valles, M., Bascompta, M., Sanmiquel, L., Escobet, T., Argelaguet, R., Escobet, A., de Felipe, J.J., Parcerisa, D., Peña-Pitarch, E. (2018). Breakage Function for HPGR: Mineral and Mechanical Characterization of Tantalum and Tungsten Ores. *Minerals*, 8, p. 170, <https://doi.org/10.3390/min8040170>.
- [11] Schönert, K. (1988). A first survey of grinding with high-compression roller mills. *Int. J. Miner. Process.*, 22, pp. 401–412. [https://doi.org/10.1016/0301-7516\(88\)90075-0](https://doi.org/10.1016/0301-7516(88)90075-0).
- [12] Yin, W., Tang, Y., Ma, Y., Zuo, W., Yao, J. (2017). Comparison of sample properties and leaching characteristics of gold ore from jaw crusher and HPGR. *Miner. Eng.*, 111, pp. 140–147. <https://doi.org/10.1016/j.mineng.2017.06.012>.

- 
- [13] Nagataa Y, Tsunazawab Y, Tsukadac K, Yaguchid Y, Ebisue Y, Mitsuhashie K, Tokorof C. (2020). Effect of the roll stud diameter on the capacity of a high-pressure grinding roll using the discrete element method, *Miner. Eng.*, 154, <https://doi.org/10.1016/j.mineng.2020.106412>
- [14] Ballantyne, G. R., Hilden, M., van der Meer, F. P. (2018). Improved characterisation of ball milling energy requirements for HPGR products. *Miner. Eng.*, 116, pp. 72–81, <https://doi.org/10.1016/j.mineng.2017.06.005>.
- [15] Liu, L., Tan, Q., Liu, L., Li, W., Lv, L. (2017). Comparison of grinding characteristics in high-pressure grinding roller (HPGR) and cone crusher (CC). *Physicochem. Probl. Miner. Process.*, 53, pp. 1009–1022. <https://doi.org/10.5277/ppmp170226>.
- [16] <https://www.aluminazv.ba/en/category-products/8>; downloaded: 01. 07. 2021.
- [17] Tavares, L. M. (2005). Particle weakening in high-pressure roll grinding. *Miner. Eng.*, 18, pp. 651–657, <https://doi.org/10.1016/j.mineng.2004.10.012>.